ACS Macro Letters

Letter

pubs.acs.org/macroletters

Bioinspired Strategy to Reinforce PVA with Improved Toughness and Thermal Properties via Hydrogen-Bond Self-Assembly

Ping'an Song,[†,‡] Zhiguang Xu,[†] and Qipeng Guo*[,†]

[†]Polymers Research Group, Institute for Frontier Materials, Deakin University, Locked Bag 2000, Geelong, Victoria 3220, Australia

[‡]Department of Materials, College of Engineering, Zhejiang Agriculture and Forestry University, Hangzhou, Zhejiang, 311300, China

Supporting Information

ABSTRACT: Despite the high strength and stiffness of polymer nanocomposites, they usually display lower deformability and toughness relative to their matrices. Spider silk features exceptionally high stiffness and toughness via the hierarchical architecture based on hydrogen-bond (H-bond) assembly. Inspired by this intriguing phenomenon, we here exploit melamine (MA) to reinforce poly(vinyl alcohol) (PVA) via H-bond self-assembly at a molecular level. Our results have shown that due to the formation of physical cross-link network based on H-bond assembly between MA and PVA, yield strength, Young's modulus, extensibility, and toughness of PVA are improved by 22, 25, 144, and 200% with 1.0 wt % MA, respectively. Moreover, presence of MA can enhance the thermal stability of PVA to a great extent, even exceeding some nanofillers (e.g., graphene). This work provides a facile method to improve the mechanical properties of polymers via H-bond self-assembly.

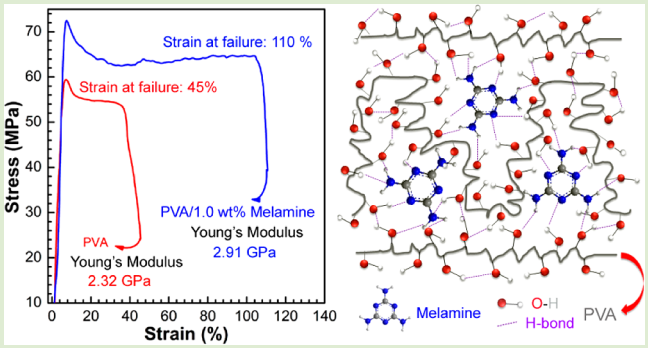

Poly(vinyl alcohol) (PVA) is commercially important hydrophilic polymer featuring many outstanding properties.[1,2] Recently, of particular interest is to improve the mechanical properties of PVA because of the high efficiency to form strong hydrogen bonds[3] and its superior capability to transfer load between the polymer and the reinforcing agents. Creating polymer nanocomposites has recently been proven to be a highly effective strategy to produce advanced composites, exhibiting remarkably enhanced thermal and mechanical properties only at a low loading of nanoparticles.[4,5] PVA has been reinforced by various nanofillers including nanodiamond,[6] carbon nanotubes (CNTs),[7−9] inorganic clay (e.g., montmorillonite),[10,11] and graphene.[5,12−14] Although these nanofillers can significantly improve its mechanical properties, they usually dramatically reduce the extensibility and toughness. Thus, it is highly attractive to improve PVA with balanced stiffness and toughness.

Biological protein materials feature multiscale hierarchical structures composed primarily of hierarchical assemblies of hydrogen bonds (H-bonds).[15] Although H-bonds are extremely weak chemical bonding, they can serve as the essential building blocks enabling biological protein materials to display extraordinary strength, robustness, and toughness.[16,17] A persuasive example is spider silk, which displays an initial modulus of ∼10 GPa,[18] a great extensibility (strain at failure ≥50%),[19] and an ultimate tensile strength of 1−2 GPa.[20] Recent research reveals that it is the highly well-organized, densely H-bonds β-sheet nanoscrystals confined to several nanometers within a semimorphous protein matrix, which enables the protein materials to exhibit the exceptional mechanical properties.[21] This charming biological phenomenon provides us a promising strategy to reinforce polymers.

Therefore, we here exploit melamine improve the mechanical properties of PVA via the H-bonding interactions, considering melamine, a simple organic molecule, but capable of forming multiple H-bonds due to six N atoms as donors and six H atoms as acceptors. The physical cross-link networks formed via H-bond self-assembly are expected to play a similar role to β-sheet nanocrystals in silk fibers by producing nanoconfinement.[21] Moreover, mixing of MA with PVA at a molecular level can be easily realized via simple solution blending.

It is essential to investigate the H-bond interactions between PVA and MA because they overwhelm all other interactions in our system and strongly affect mechanical properties of resultant materials. As shown in Figure 1A, pure PVA shows a typically sharp and broad absorption band at 3000−3600 cm^{-1} centering at 3281 cm^{-1}, arising from the stretching vibration of hydroxyl groups (O−H) due to extensively intermolecular/intramolecular H-bond interactions for that of free hydroxyls of secondary alcohols is usually only observed at ∼3620 cm^{-1}.[1,22,23] The neighboring strong absorption peaks at 2936 and 2907 cm^{-1} are attributed to the stretching vibrations of methylene groups. For MA, two absorption peaks at 3468 and 3418 cm^{-1} are observed, which are attributed to the

Received: October 19, 2013
Accepted: December 5, 2013
Published: December 6, 2013

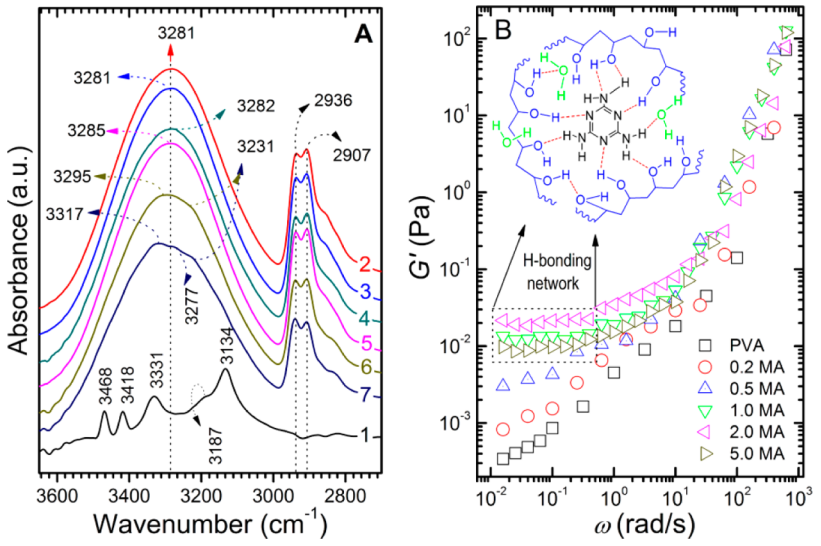

Figure 1. (A) IR spectra, stretching of O−H of (1) MA, (2) PVA, (3) 0.2 MA, (4) 0.5 MA, (5) 1.0 MA, (6) 2.0 MA, and (7) 5.0 MA (3000−3500 cm^{-1}), and (B) frequency dependence of dynamic storage modulus (G') for 8.0 wt % aqueous solution of PVA and its blends with MA.

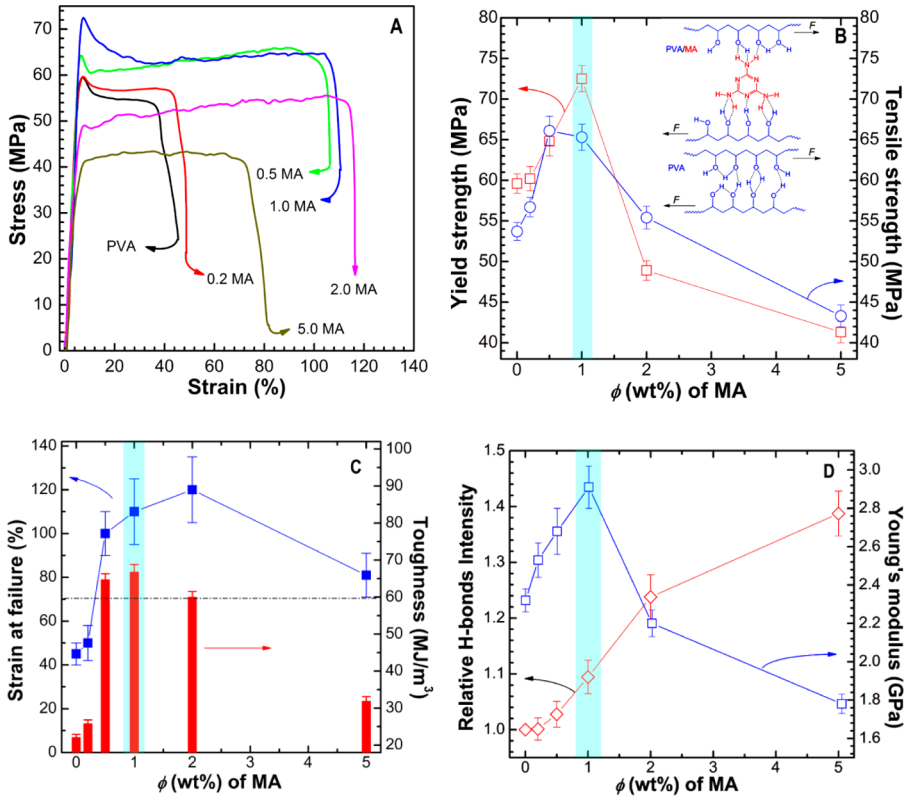

Figure 2. (A) Typical stress−strain curves: plots of (B) yield strength and tensile strength, (C) strain at failure and tensile toughness at failure, and (D) H-bond density and Young's modulus for PVA and its blends as a function of MA content.

stretching vibrations of free N−H. The stretching vibrations of H-bonding N−H are shown at 3331, 3187 (weak), and 3134 cm^{-1}.[24−26] For 0.2 MA, the number of H-bond is too low to be determined by IR spectra. Upon the MA loading exceeding 0.2 wt %, the peak position of the stretching vibration of H-bonded O−H groups is gradually shifted to high frequency with increasing MA content accompanied by the occurrence of new types of H-bonds producing different absorption peaks. The peak position is notably increased from 3281 cm^{-1} (for PVA and 0.2 MA) to 3282 cm^{-1} for 0.5 MA, then to 3285 cm^{-1} for 1.0 MA, followed by 3295 cm^{-1} for 2.0 MA and 3317 cm^{-1} for 5.0 MA due to the participation of the H-bonds interacted with more N atoms.[1,24,25] Additionally, one new weak peak appears at 3231 cm^{-1} (N−H···O) when the content of MA is 2.0 wt %. When the content of MA increased to 5.0 wt %, another new weak peak emerges at 3277 cm^{-1} assigned to the intramolecular H-bonding in PVA molecules, probably because the presence of MA weakens the intermolecular interaction of PVA, and consequently increases the probability of intramolecular H-bonding. Moreover, the strong H-bonding interactions between

dx.doi.org/10.1021/mz4005265 | ACS Macro Lett. 2013, 2, 1100−1104

PVA and MA can also be evidenced by the changes in the absorptions of both N−H and C−N groups (Supporting Information, Figure S3).

Rheological tests allow us to evaluate the intermolecular interactions of polymer with other components.[27] Figure 1B shows that the slope of plotting log G' versus log ω for pure PVA is only 0.65 in low ω region, which significantly deviates the classical linear viscoelastic relationship of log G' $(\omega) \sim 2$ log ω in the terminal region[28] due to the existence of extensive intermolecular H-bonding interactions. Generally, the slope depress is due to the network growing and forming, while the increase in G' at low frequencies reflect the extent of network formation.[27] The slope gradually reduces with increasing MA content, with a slope of 0.60 for 0.2 MA and 0.40 for 0.5 MA, respectively. Meanwhile, G' also increases with increasing MA content, clearly indicating the growing of physical cross-link network due to strong H-bonding interactions between MA and PVA, despite of the presence of H_2O. Moreover, for 1.0 MA G' dramatically increases but the slope almost close to zero, and a so-called "second platform" or "solid-like" behavior appears in the terminal region. This platform is believed as the formation of the physical cross-link network with MA molecules acting as cross-link sites by multiple H-bond self-assembly.[27] This "solid-like" behavior has widely been observed in polymer composites filled with CNTs and clay.[29−32] However, the platform value of G' reaches the peak for 2.0 MA and then decreases for 5.0 MA, even below the value of 1.0 MA. This phenomenon is also observed in loss modulus (G''), complex viscosity (η^*), and apparent viscosity (η) (see Supporting Information, S4).

Similar to rheological behavior, all mechanical parameters are increased and then reduced with increasing MA concentration (see Figure 2). PVA displays a yield strength of 59.2 MPa, tensile strength of 53.9 MPa, Young's modulus of 2.32 GPa, strain at failure of about 45% and a tensile toughness of about 22.0 MJ/m^3. Addition of 0.2 wt % MA only leads to limited improvements in mechanical properties. However, when the MA content reaches 1.0 wt %, almost all mechanical parameters achieve the maximum values. The yield strength and Young's modulus are increased up to 72.3 MPa and 2.91 GPa, respectively, 22 and 25% higher than those of pure PVA (see Figure 2B,D). Dynamic mechanical analysis also shows comparable improvements in storage modulus (Supporting Information, Figure S5 and Table S1). These enhancements in strength and modulus even approach the values achieved by means of incorporating equal loading nanofillers into PVA.[2,8,33] Moreover, both the strain at failure and toughness are remarkably improved by 144 and 200%, respectively (Figure 2C), which is likely due to the destruction and reconstruction of large numbers of H-bonding in PVA/MA systems since H-bonding groups are able to rebuild to self-heal the overall H-bonding network structure during a slow deformation process.[34] Both strength and deformability of the hydrogels were steadily enhanced with increasing 2-vinyl-4,6-diamino-1,3,5-triazine (a MA derivative) content due to the formation of strong H-bonding network.[34] Liu et al. recently observed nearly 100% increases in both tensile strength and modulus but a ∼70% reduction in elongation at break of PVA modified by borate.[35] Just recently, Burghard et al.[36] has also reported that H_2O molecules between layers remarkably improve both stiffness and toughness of V_2O_5 nanofiber paper via the formation of H-bond network. Meanwhile, H-bond networks assembled by water molecules have been found to be able to affect and even control the stiffness of graphene oxides paper-like materials and its associated polymer nanocomposites.[37,38] Hence, the observed considerably mechanical improvements are primarily attributed to the strong H-bond networks serving as the action of nanoconfinement.

However, further increasing the MA concentration (above 1.0 wt %) deteriorates the strength and modulus instead of causing continuous enhancement, even if the viscoelastic tests shows that 2.0 wt % is the optimum content for MA to form densely physical cross-link network via H-bonding assembly with PVA. This suggests that the response of mechanical failure deviates from the theoretical predication. Actually, the physical cross-link network has been established at 1.0 wt % of MA (Figure 2A). In addition, the viscoelastic tests were performed in aqueous solution, which is quite different from the tensile tests for the samples of the latter hardly contain water. Although more MA at high concentration will participate in the formation of H-bond interactions, it probably simultaneously generates the plasticization effects to some degree for MA is a small molecule. The plasticization effect can be reflected by the high elongation at break for both 2.0 and 5.0 MA, still higher than that of PVA.

To further investigate the relationship between the H-bonding density or strength and the Young's modulus, we take the absorption peak of the methylene group (2983−2770 cm^{-1}) as the inner reference and compare the area of absorption peak of H-bond stretching (3600−2985 cm^{-1}) with the area of the former. Figure 2D shows that the relative H-bond intensity gradually increases with increasing MA concentration, which is well consistent to Young's modulus change at low MA content but deviates gradually when MA content is above 1.0 wt % due to the plasticization effects of MA.

DSC and TGA measurements were carried out to determine the effects of the H-bonding assembly on the thermal properties. As can be seen from Table 1 and DSC curves (see Supporting Information, Figure S6), neat PVA exhibits a glass transition temperature (T_g) of 78.4 °C, a melting point (T_m) of 217.3 °C and a degree of crystallinity (χ_c) of 35.4% if one takes 138.6 J/g as the melting enthalpy (ΔH_f^0) of 100% crystalline PVA.[39] The T_gs values are gradually increased but T_m monotonously decreased with increasing MA concentration, which can also observed by dynamic mechanical analysis (Supporting Information, Table S1). For instance, 5.0 MA displays a T_g of 84.3 °C, which is 5.9 °C higher than that of PVA matrix, and a T_m of 212.0 °C, about 5.3 °C lower than that of neat PVA. Li et al. reported only a slight increase in T_g of

Table 1. Experimental Formulations and Detailed Data Obtained from DSC Tests

run	PVA (wt %)	MA (wt %)	T_g[a] (°C)	T_m[a] (°C)	ΔH_f[a] (J/g)	χ_c[a] (%)
PVA	100	0	78.4	217.3	49.0	35.4
0.2 MA	99.8	0.20	78.7	216.1	45.5	32.8
0.5 MA	99.5	0.50	80.1	215.2	44.2	31.9
1.0 MA	99.0	1.00	81.5	214.4	42.7	30.8
2.0 MA	98.0	2.00	83.4	213.2	40.6	29.3
5.0 MA	95.0	5.00	84.3	212.0	48.2	34.8
10.0 MA	90.0	10.0	85.8	211.3	50.6	36.3

[a] T_g refers to the glass transition temperature while ΔH_f and χ_c represent the melting enthalpy and degree of crystallinity, respectively.

dx.doi.org/10.1021/mz4005265 | ACS Macro Lett. 2013, 2, 1100−1104

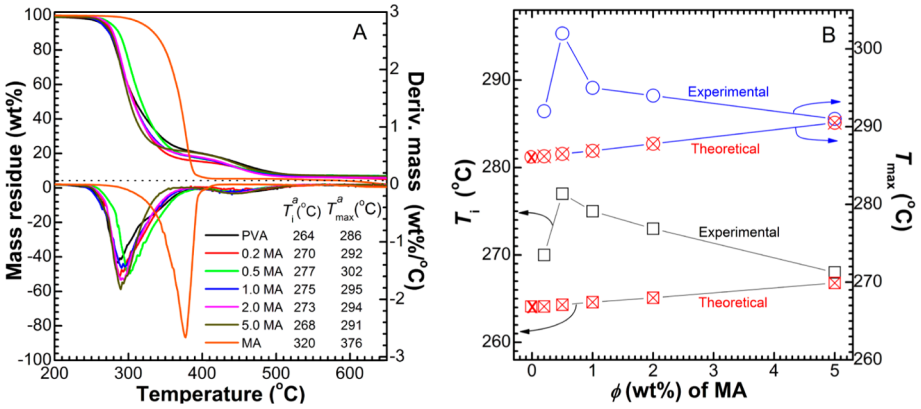

Figure 3. (A) TGA/DTG curves and (B) comparison of experimental values to theoretical values of degradation temperatures of PVA and its blends of MA in N_2 condition. T_i and T_{max} refer to the temperature where 5 wt % mass loss and maximum mass loss rate take place.

PVA from 76 to 78 °C with 1.0 wt % SWNTs[40] and even 1.6 wt % graphene was also found to delay the T_g of PVA only by 3.1 °C,[41] while 1.0 wt % MA makes the T_g value increased by 3.1 °C in our system.

The T_gs enhancements observed here are primarily due to the strong H-bonding interactions between MA and PVA will restrict the free movements and arrangement of PVA chains. As for the depression of T_m, it is closely related to the degree of crystallity and it is normal for T_ms change since the latter reduces with increasing MA content. However, 5.0 MA gives a much high χ_c of 34.8%, even approaching 35.4% for PVA matrix. Meanwhile, a higher χ_c of 36.3% is also observed for 10.0 MA (only taking the transparent part of the film for test, avoiding the MA points separated, see Supporting Information, Figure S1). This rebound in χ_c is similar to its viscoelastic behavior, probably because that higher MA content above 2.0 wt % enables MA to form small aggregates via H-bond interactions among themselves. The aggregates may act as the nucleating agent like graphene[12] for PVA and consequently increase the degree of crystallinity.

As shown in Figure 3A, PVA matrix starts to degrade at about 264 °C (T_i) and experiences the rapidest decomposition (T_{max}) at ~286 °C. MA is relatively thermally stable showing a T_i of 320 °C and a T_{max} of 376 °C. Unexpectedly, both T_i and T_{max} of PVA are enhanced to some extent upon introducing MA, and their peak values of 277 and 302 °C occur for 0.5 MA, which are 13 and 16 °C higher than corresponding value of PVA. The 0.7 wt % of graphene oxides were reported to increase them of PVA only by 3 and 5.5 °C, respectively.[12] Another research showed that adding 1.6 wt % graphene led to a ~10 °C increase in T_{max} and hardly contributed to the T_i of PVA under the same condition.

To study the effects of H-bonds on thermal stability, we assume that thermal stability parameters (T_i and T_{max}) obey the linear mixing law, namely, expressed by eq 1:

$$T_b = \phi_P T_P + \phi_M T_M \quad (1)$$

where T_b, T_P, and T_M, respectively, represent the special temperature of polymer blend, pure polymer (here, PVA), and pristine filler (here, MA), and ϕ_P and ϕ_M refer to the mass fraction of PVA and MA. As presented in Figure 3B, all experimental values of both T_i and T_{max} are much higher than the theoretical values of them calculated by above linear law except for 5.0 MA. The 0.5 MA exhibits the largest differences between experimental values and theoretical ones, which in turn indicate that the strong H-bond interactions play the key role in the improved thermal stability, making it deviate from the linear mixing law. However, 5.0 MA gives a T_i of 268 °C and a T_{max} of 291 °C, which are quite close to their corresponding values, 266.8 and 290.5 °C. This interesting finding clearly suggests that once the concentration of MA exceeds 2.0 wt %, the H-bond interactions among MA itself will overwhelm its interactions with PVA, as a consequence making their mixing nearly obey the linear mixing rule. This is perfectly consistent to the deviation behaviors of the rheological, mechanical and the rebound of χ_c observed above.

In conclusion, we have successfully adopted a facile approach to achieve balanced stiffness and toughness as well as extensibility. Only adding small amount (1.0 wt %) of MA is able to significantly improve the strength, modulus, extensibility and toughness of PVA due to the formation of physical cross-link network via H-bond self-assembly. In addition, the H-bond network can also enhance the thermal stability of PVA to a great extent. This work opens the door toward biomimetic reinforcement for polymeric materials of high stiffness and toughness via creating H-bond network using small organic molecules as building blocks.

■ ASSOCIATED CONTENT

Supporting Information

Materials, sample preparation, and characterization. This material is available free of charge via the Internet at http://pubs.acs.org.

■ AUTHOR INFORMATION

Corresponding Author

*E-mail: qguo@deakin.edu.au.

Notes

The authors declare no competing financial interest.

■ ACKNOWLEDGMENTS

P.S. was supported by the Alfred Deakin Postdoctoral Research Fellowship Scheme and by the National Science Foundation of China (Grant No. 51303162).

■ REFERENCES

(1) Buslov, D. K.; Sushko, N. I.; Tretinnikov, O. N. *Polym. Sci., Ser. A* **2011**, *53*, 1121−1127.

(2) Zhou, K. Q.; Jiang, S. H.; Bao, C. L.; Song, L.; Wang, B. B.; Tang, G.; Hu, Y.; Gui, Z. *RSC Adv.* **2012**, *2*, 11695−11703.

(3) Zhang, H. J.; Xia, H. S.; Zhao, Y. *ACS Macro Lett.* **2012**, *1*, 1233−1236.
(4) Zanetti, M.; Camino, G.; Reichert; MÜlhaupt, P. R. *Marcomol. Rapid Commun.* **2001**, *22*, 176−180.
(5) Potts, J. R.; Dreyer, R. D.; Bielawski, C. W.; Ruoff, R. S. *Polymer* **2011**, *52*, 5−25.
(6) Morimune, S.; Kotera, M.; Nishino, T.; Goto, K.; Hata, K. *Macromolecules* **2011**, *44*, 4415−4421.
(7) Beese, A. M.; Sakar, S.; Nair, A.; Naraghi, M.; An, Z.; Moravsky, A.; Loutfy, R. O.; Buehler, M. J.; Nguyen, S. T.; Espinosa, H. D. *ACS Nano* **2013**, *7*, 3434−3446.
(8) Liu, L. Q.; Barner, A. H.; Nuriel, S.; Wagner, H. D. *Adv. Funct. Mater.* **2005**, *15*, 975−980.
(9) Shim, B. S.; Zhu, J.; Jan, E.; Critchley, K.; Ho, S.; Podsiadlo, P.; Sun, K.; Kotov, N. A. *ACS Nano* **2009**, *3*, 1711−1722.
(10) Podsiadlo, P.; Kaushik, A. K.; Arruda, E. M.; Waas, A. M.; Shim, B. S.; Xu, J. D.; Nandivada, H.; Pumplin, B. G.; Lahann, J.; Ramamoorthy, A.; Kotov, N. A. *Science* **2007**, *318*, 80−83.
(11) Wang, J. F.; Cheng, Q. F.; Lin, L.; Chen, L. F.; Jiang, L. *Nanoscale* **2013**, *5*, 6356−6362.
(12) Liang, J. J.; Huang, Y.; Zhang, L.; Wang, Y.; Ma, Y. F.; Guo, T. Y.; Chen, Y. S. *Adv. Funct. Mater.* **2009**, *19*, 2297−2302.
(13) Zhao, X.; Zhang, Q. H.; Chen, D. J.; Lu, P. *Macromolecules* **2010**, *43*, 2357−2363.
(14) Yang, X. M.; Li, L.; Shang, S. M.; Tao, X. M. *Polymer* **2010**, *51*, 3431−3435.
(15) Keten, S.; Buehler, M. J. *Nano Lett.* **2008**, *8*, 743−748.
(16) Buehler, M. J. *Nano Today* **2010**, *5*, 379−383.
(17) Giesa, T.; Arslan, M.; Pugno, N. M.; Buehler, M. J. *Nano Lett.* **2011**, *11*, 5038−5046.
(18) Swanson, B. O.; Anderson, S. P.; DiGiovine, C.; Ross, R. N.; Dorsey, J. P. *Integr. Comp. Biol.* **2009**, *49*, 21−31.
(19) Vollrath, F.; Knight, D. P. *Nature* **2001**, *410*, 541−548.
(20) Gosline, J. M.; Denny, M. W.; Demont, M. E. *Nature* **1984**, *309*, 551−552.
(21) Keten, S.; Xu, Z. P.; Ihle, B.; Buehler, M. J. *Nat. Mater.* **2010**, *9*, 359−367.
(22) Bellamy, L. J. *The Infrared Spectra of Complex Molecules*; :Methuen: London, 1957; Inostrannaya Literatura: Moscow, 1963.
(23) Dai, L. X.; Ying, L. N. *Macromol. Mater. Eng.* **2002**, *287*, 509−514.
(24) Jones, W. J.; Orville-Thomas, W. J. *Trans. Faraday Soc.* **1959**, *55*, 203−210.
(25) Sawodny, W.; Niedenzu, K.; Dawson, J. W. *J. Chem. Phys.* **1966**, *45*, 3155−&.
(26) Wiles, A. B.; Bozzuto, D.; Cahill, C. L.; Pike, R. D. *Polyhedron* **2006**, *25*, 776−782.
(27) Wu, Q.; Shangguan, Y. G.; Du, M.; Zhou, J. P.; Song, Y. H.; Zheng, Q. *J. Colloid Interface Sci.* **2009**, *339*, 236−242.
(28) Ferry, J. D. *Viscoelastic Properties of Polymer*; New York: John Wiley, 1980.
(29) Du, M.; Gong, J. H.; Zheng, Q. *Polymer* **2004**, *45*, 6275−6730.
(30) Kashiwagi, T.; Du, F. M.; Douglas, J. F.; Winey, K. I.; Harris, R. H.; Shields, J. R. *Nat. Mater.* **2005**, *4*, 928−933.
(31) Mizuno, C.; Hohn, B.; Okamoto, M. *Macromol. Mater. Eng.* **2013**, *298*, 400−411.
(32) Leroux, F.; Illaik, A.; Stimfling, T.; Troutier-Thuilliez, A. L.; Fleutot, S.; Martinez, H.; Cellier, J.; Verney, V. *J. Mater. Chem.* **2010**, *20*, 9484−9494.
(33) Johnsy, G.; Datta, K. K. R.; Sajeevkumar, V. A.; Sabapathy, S. N.; Bawa, A. S.; Eswaramoorthy, M. *ACS Appl. Mater. Interfaces* **2009**, *1*, 2796−2803.
(34) Zhang, J. L.; Wang, N.; Liu, W. G.; Zhao, X. L.; Lu, W. *Soft Matter* **2013**, *9*, 6331−6337.
(35) Liu, L. Q.; Gao, Y.; Liu, Q.; Kuang, J.; Zhou, D.; Ju, S. T.; Han, B. H.; Zhang, Z. H. *Small* **2013**, *9*, 2466−2472.
(36) Burghard, Z.; Leineweber, A.; Van Aken, P. A.; Dufaux, T.; Burghard, M.; Bill, J. *Adv. Mater.* **2013**, *25*, 2468−2473.
(37) Medhekar, N. V.; Ramasubramaniam, A.; Ruoff, R. S.; Shenoy, V. B. *ACS Nano* **2010**, *4*, 2300−2306.
(38) Compton, O. C.; Cranford, S. W.; Putz, K. W.; An, Z.; Brinson, L. C.; Buehler, M. J.; Nguyen, S. T. *ACS Nano* **2012**, *6*, 2008−2019.
(39) Su, J. X.; Wang, Q.; Su, R.; Wang, K.; Zhang, Q.; Fu, Q. *J. Appl. Polym. Sci.* **2008**, *107*, 4070−4075.
(40) Li, C. Y.; Lv, X. F.; Dai, J. J.; Cui, J.; Yan, Y. H. *Polym. Adv. Technol.* **2013**, *24*, 376−382.
(41) Bao, C. L.; Guo, Y. Q.; Song, L.; Hu, Y. *J. Mater. Chem.* **2011**, *21*, 13942−13950.